Dye lasing in optically manipulated liquid aerosols

Y. Karadag,[1] M. Aas,[1] A. Jonáš,[1,4] S. Anand,[2] D. McGloin,[2,5] and A. Kiraz[1,3,*]

[1]*Department of Physics, Koç University, Rumelifeneri Yolu, Sariyer, Istanbul 34450, Turkey*

[2]*Electronic Engineering and Physics Division, University of Dundee, Nethergate, Dundee DD1 4HN, UK*

[3]*Koç University TÜPRAŞ Energy Center (KÜTEM), Koç University, Rumelifeneri Yolu, Sariyer, Istanbul 34450, Turkey*

[4]*e-mail: ajonas@ku.edu.tr*

[5]*e-mail: d.mcgloin@dundee.ac.uk*

**Corresponding author: akiraz@ku.edu.tr*

Received March 11, 2013; revised April 5, 2013; accepted April 5, 2013;
posted April 9, 2013 (Doc. ID 186719); published May 10, 2013

We report lasing in airborne, rhodamine B-doped glycerol–water droplets with diameters ranging between 7.7 and 11.0 μm, which were localized using optical tweezers. While being trapped near the focal point of an infrared laser, the droplets were pumped with a *Q*-switched green laser. Our experiments revealed nonlinear dependence of the intensity of the droplet whispering gallery modes (WGMs) on the pump laser fluence, indicating dye lasing. The average wavelength of the lasing WGMs could be tuned between 600 and 630 nm by changing the droplet size. These results may lead to new ways of probing airborne particles, exploiting the high sensitivity of stimulated emission to small perturbations in the droplet laser cavity and the gain medium. © 2013 Optical Society of America

OCIS codes: (140.3945) Microcavities; (140.2050) Dye lasers; (010.1110) Aerosols; (350.4855) Optical tweezers or optical manipulation; (300.2530) Fluorescence, laser-induced.

http://dx.doi.org/10.1364/OL.38.001669

Owing to the liquid surface tension, micron-sized droplets assume the shape of perfect spheres that can serve as natural optical resonant cavities hosting high-quality whispering gallery modes (WGMs). Enhanced optical fields and small modal volumes of such WGMs then facilitate the observation of nonlinear optical phenomena at incident power thresholds that are significantly lower than those required for bulk samples. Easy access to the regime of nonlinear optical response in the droplets enables precise characterization of the droplet size and material properties via cavity-enhanced Raman spectroscopy [1] and building of microscopic lasers based on liquid cavities containing a gain medium [2]. Such droplet-based microlasers have already found applications in biological and chemical sensing [3,4]. In addition, the possibility of readily adjusting the shape, size, and composition of liquid microcavities opens up the way toward controlled tuning of the emission spectral characteristics of liquid microlasers [5,6].

Lasing in airborne microdroplets was first successfully demonstrated almost 30 years ago in freely flowing streams of droplets [7]. However, freely moving liquid aerosols have only a limited use in practical applications in sensing and microlaser design. In order to fully exploit the potential of lasing WGMs in microdroplets, it is necessary to stabilize the droplet position over extended time periods. The position stabilization of droplets of water and other polar liquids can be effectively realized by depositing them on a superhydrophobic surface [8]. Active, noninvasive control of the droplet position by external micromanipulation then represents the next step in the practical exploitation of lasing aerosols. To date, manipulation of lasing airborne microdroplets has been demonstrated in electrodynamic [9] and acoustic [10] trapping configurations. Optical tweezing is another micromanipulation technique that is especially well suited for stable confinement of very small droplets and readily adaptable for simultaneous manipulation of large numbers of particles [11]. Various studies employed optical tweezing to localize liquid aerosols over long periods of time for applications in a large variety of fields including atmospheric chemistry and physics, and health science [12,13]. Optical tweezing has also been used to confine and move solid lasing microspheres [14] or lasing emulsion droplets [15]. However, up to now lasing has not been demonstrated in liquid aerosols manipulated using optical tweezers.

In this Letter, we report lasing from individual optically trapped liquid aerosol particles doped with a fluorescent dye. We characterize the droplet emission spectrum as a function of the droplet size and show that the droplet lasing wavelength can be tuned over an interval larger than 30 nm by adjusting the droplet radius.

Optical setup used for the experiments with trapped aerosol lasing was described previously [15]. A continuous wave solid state infrared laser ($\lambda = 1064$ nm, 300 mW maximum power; Crystalaser) was used for aerosol trapping. The trapping laser beam was sent through a beam expander and focused into the sample chamber by a water immersion microscope objective (NA = 1.2, 60×; Nikon) in the inverted microscope geometry. Based on the previous work [13], the power of the trapping beam was set to 3.5 mW at the focus of the microscope objective for stable on-axis trapping of aerosols with diameters ranging between 5 and 10 μm. Pulsed green beam ($\lambda = 532$ nm, 20 ns pulse width and 33 kHz repetition rate) obtained after frequency-doubling the output of a home-built, passively *Q*-switched Nd-YVO_4 laser was used for pumping the trapped microdroplets. The pump beam was delivered to the setup through a multimode fiber, combined with the trapping beam by a dichroic mirror, and focused by the same microscope objective that was employed for optical trapping to a 9.8 μm diameter spot. In our experiments, the trapping and pump beams were focused at the same plane approximately 20 μm above the upper surface of the cover glass that formed the bottom part of the sample chamber. For efficient excitation of WGMs in the trapped droplet by on-edge

optical pumping, the focal spot of the pump beam was approximately centered at the rim of the droplet. The fluorescence emission from the droplets was collected using the same microscope objective and dispersed by a monochromator (focal length 500 mm; Acton Research) on the chip of a cooled CCD detector (Pixis 100; Princeton Instruments). In order to prevent fast photobleaching of the dye molecules in the droplets, a shutter was added to the pump laser beam path. This shutter was synchronized with the CCD detector and triggered the spectrum acquisition during an exposure time of 10 ms.

A compact ultrasonic nebulizer (JIH50; Beuer) was used for generating liquid aerosols out of 39% w/w glycerol/water solution (refractive index $n_{\text{int}} = 1.38$, density $\rho = 1.099\ \text{g/cm}^3$) doped with 1 mM rhodamine B dye. The nebulizer was attached to a closed glass sample chamber that prevented external air flow from disturbing the stability of the trapped aerosol particles and maintained approximately constant ambient humidity during the experiments. A cover glass treated with Ar/O_2 plasma was attached at the bottom of the sample chamber. Plasma cleaning of cover glasses ensured a good hydrophilicity of their surface, thus preventing accumulation of large sessile droplets that otherwise disturb the trapping and pump beams focused into the chamber. During the experiments, initial diameters of the trapped droplets were generally around 5 μm. Larger droplets were then obtained by fusion of the trapped droplets with others that were attracted to the trapping region. Trapped droplet diameters were estimated from microscope images and independently determined from the observed WGM free-spectral range (FSR), mean lasing wavelength $\bar{\lambda}$, and known refractive indices of the droplet ($n_{\text{int}} = 1.38$) and air ($n_{\text{ext}} = 1.00$), using the asymptotic formula of Chylek *et al.* [16].

Figure 1 shows fluorescence emission spectra recorded from a trapped 9.4 μm diameter glycerol/water aerosol droplet at varying excitation fluences. Nonlasing WGMs of the aerosol particle were observed in Fig. 1(a) when the excitation fluence was lower than the lasing threshold. These WGMs are superimposed on a broad nonresonant background emission from the dye-doped thin solution layer formed on the cover glass during the experiment. In general, droplet WGMs can be characterized using radial, azimuthal, and angular mode numbers, and polarization (TE or TM) [6]. The WGMs that belong to the same mode family with identical radial mode number and polarization are indicated in Fig. 1(a). Spectral separation between two such consecutive WGMs gives the FSR, which is equal to 10.7 nm. In order to observe lasing, the cavity losses must be smaller than the net cavity gain. Excitation fluence and the amount of dye in the aerosol particle are critical to satisfy this condition. As shown in Figs. 1(b) and 1(c), two WGMs denoted as A and B exhibit lasing around $\lambda = 608$ nm and $\lambda = 618$ nm upon crossing the threshold excitation fluences of $0.76\ \text{mJ/cm}^2$ and $0.84\ \text{mJ/cm}^2$. Owing to the very low volatility of glycerol and approximately stabilized relative humidity in the sample chamber, the spectral positions of lasing WGMs display only a minimal drift $\Delta\lambda = 0.06$ nm over the total duration of the experiment (2 min). For a droplet with the mean radius $a = 4.7$ μm,

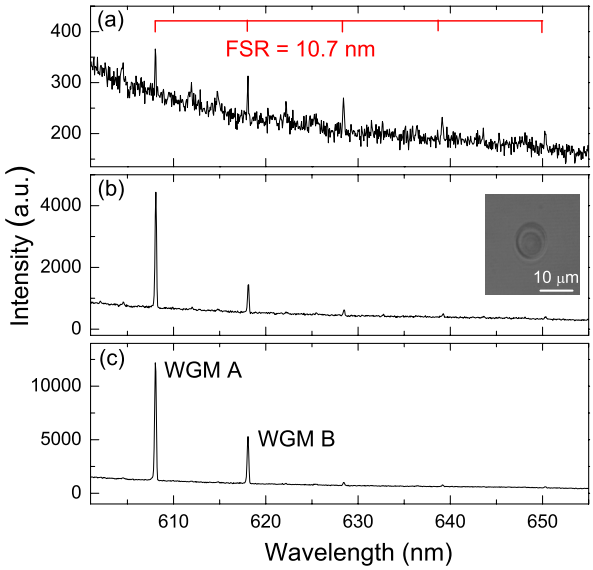

Fig. 1. Excitation fluence-dependent emission spectra recorded from a 9.4 μm diameter glycerol/water droplet at three different excitation fluences: (a) $0.49\ \text{mJ/cm}^2$, (b) $1.70\ \text{mJ/cm}^2$, and (c) $3.06\ \text{mJ/cm}^2$. WGM A and WGM B denote lasing WGMs. Inset: optical microscope image of the trapped lasing droplet.

this translates into the drift of the droplet radius by $\Delta a = \Delta\lambda(a/\lambda) = 0.46$ nm.

Figure 2 displays the intensities of the lasing WGMs A and B indicated in Fig. 1 and nonresonant spectral background in the vicinity of these WGMs as a function of the excitation fluence. Both lasing and background intensities were determined from Lorentzian fits to WGMs in a series of emission spectra acquired with gradually increasing excitation fluence. Subsequently, two lines were fitted to the respective lasing and background intensity series and the intersection of the fitted lines provided the threshold excitation fluences of $0.76\ \text{mJ/cm}^2$ and $0.84\ \text{mJ/cm}^2$ for WGM A and WGM B, respectively [15]. As expected, the background intensity increased linearly with the excitation fluence; this also indicated that the photobleaching effects during the acquisition of the excitation fluence-dependent spectral series could be

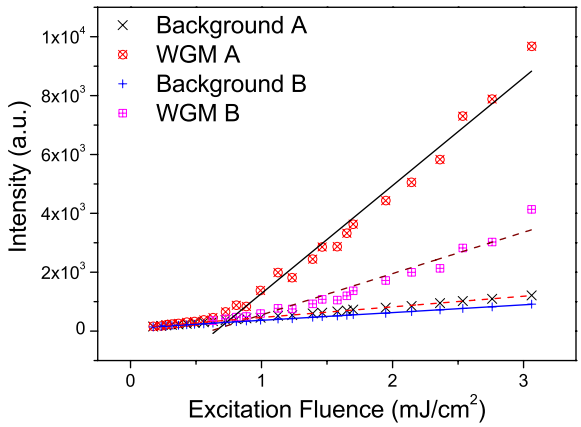

Fig. 2. Excitation fluence-dependent intensities of the lasing WGMs and background emissions in a 9.4 μm diameter glycerol/water aerosol droplet.

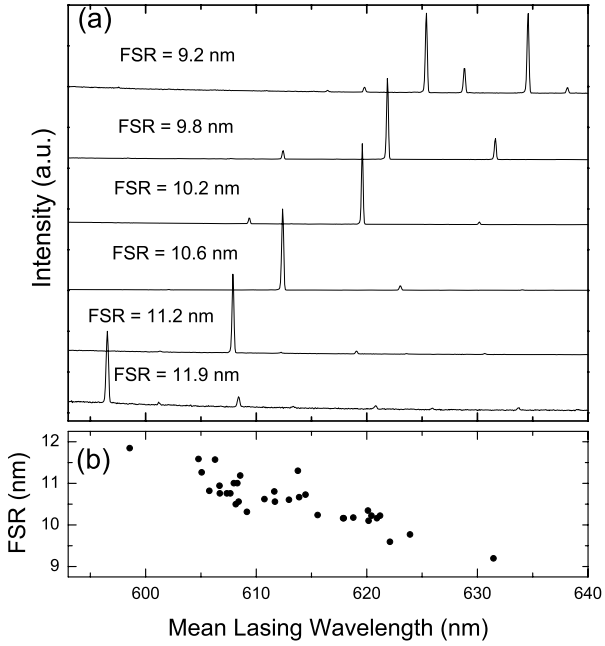

Fig. 3. (a) Lasing spectra recorded from six different aerosols with diameters 7.7, 8.4, 9.0, 9.6, 10.1, and 11.0 μm (bottom to top) at constant excitation fluence of 2.41 mJ/cm^2. (b) Free spectral ranges of 34 lasing aerosols as a function of the mean lasing wavelength, $\bar{\lambda}$.

neglected owing to the short exposure time required for recording individual spectra. When the excitation fluence exceeded the threshold, increase of the intensity of the lasing peak with a higher slope relative to the background emission indicated the onset of lasing. The threshold excitation fluence depends on the size of the trapped aerosol particle and the Q-factor of its WGMs [17]. Large radiative losses in smaller droplets result in an exponential decrease of their WGM Q-factors [18]. This sets a lower limit to the diameter of droplets that display lasing at a given maximal excitation fluence. In our experimental conditions, this lower limit was determined as 7.7 μm.

With increasing droplet size, spectral position of the emission maximum of lasing aerosols containing constant dye concentration was observed to shift to longer wavelengths. This trend is illustrated in Fig. 3(a), which shows emission spectra of six droplets with different radii recorded at fixed 2.41 mJ/cm^2 excitation fluence. Here, the increasing droplet radius corresponds to the decreasing FSR of the droplet [16]. For the given droplet, spectral location of its overall maximal lasing gain can be quantitatively characterized by the mean lasing wavelength $\bar{\lambda}$ calculated as the intensity-weighted average of the wavelengths of all lasing WGMs from the same mode family observed in the droplet's spectrum. Figure 3(b) summarizes the relationship between $\bar{\lambda}$ and FSR for 34 lasing droplets of varied size. Within the studied range of droplet sizes (7.7–11.0 μm), FSR decreased with $\bar{\lambda}$ following an almost linear dependence. A similar spectral shift of the overall lasing gain profile was previously observed in lasing emulsion droplets [6,15] and explained by the size-dependence of the efficiency of light outcoupling from the droplets and the cross section of the lasing WGMs.

We have demonstrated lasing in the WGMs of dye-doped glycerol/water microdroplets manipulated in air using optical tweezers. By changing the trapped droplet size, we have shown that the average lasing wavelength could be tuned between 600–630 nm. Controlled fusion of multiple droplets confined in dynamically positioned independent optical traps, manipulation of relative humidity and temperature in the sample chamber, or local heating with the trapping laser can be further used for precise control of the lasing droplet size. Our results are readily adaptable to simultaneous manipulation of large numbers of lasing aerosol particles. They also bring up the possibility of using the high sensitivity of stimulated emission to small perturbations in the shape, size, and material properties of the droplet cavity for sensitive chemical and biological analysis in airborne particles.

This work was partially supported by TÜBİTAK (Grant No. 111T059). S.A. thanks the Schlumberger Faculty for the Future program for support.

References

1. J. P. Reid, H. Meresman, L. Mitchem, and R. Symes, Int. Rev. Phys. Chem. **26**, 139 (2007).
2. K. Mølhave, A. Kristensen, and N. A. Mortensen, *Advanced Photonic Structures for Biological and Chemical Detection* (Springer, 2009), pp. 471–486.
3. M. Tanyeri and I. M. Kennedy, Sensor Lett. **6**, 326 (2008).
4. M. Humar and I. Musevic, Opt. Express **19**, 19836 (2011).
5. M. Humar, M. Ravnik, S. Pajk, and I. Musevic, Nat. Photonics **3**, 595 (2009).
6. S. K. Y. Tang, R. Derda, Q. Quan, M. Loncar, and G. M. Whitesides, Opt. Express **19**, 2204 (2011).
7. H.-M. Tzeng, K. F. Wall, M. B. Long, and R. K. Chang, Opt. Lett. **9**, 499 (1984).
8. A. Kiraz, A. Sennaroglu, S. Doganay, M. A. Dundar, A. Kurt, H. Kalaycoglu, and A. L. Demirel, Opt. Commun. **276**, 145 (2007).
9. M. Tona and M. Kimura, J. Phys. Soc. Jpn. **69**, 3533 (2000).
10. H. Azzouz, L. Alkhafadiji, S. Balslev, J. Johansson, N. A. Mortensen, S. Nilsson, and A. Kristensen, Opt. Express **14**, 4374 (2006).
11. D. R. Burnham and D. McGloin, Opt. Express **14**, 4176 (2006).
12. R. J. Hopkins, L. Mitchem, A. D. Ward, and J. P. Reid, Phys. Chem. Chem. Phys. **6**, 4924 (2004).
13. D. McGloin, D. R. Burnham, M. D. Summers, D. Rudd, N. Dewar, and S. Anand, Faraday Discuss. **137**, 335 (2008).
14. K. Sasaki, H. Fujiwara, and H. Masuhara, Appl. Phys. Lett. **70**, 2647 (1997).
15. M. Aas, A. Jonáš, and A. Kiraz, Opt. Commun. **290**, 183 (2013).
16. P. Chylek, J. T. Kiehl, and M. K. W. Ko, Phys. Rev. A **18**, 2229 (1978).
17. A. J. Campillo, J. D. Eversole, and H. B. Lin, Phys. Rev. Lett. **67**, 437 (1991).
18. A. Serpengüzel, J. C. Swindal, R. K. Chang, and W. P. Acker, Appl. Opt. **31**, 3543 (1992).